T-AM-SymII-1 MOLECULAR AND CELLULAR GRAPHICS AT THE NIH
Richard J. Feldmann, Division of Computer Research and Technology
National Institutes of Health, Bethesda, Maryland 20205

The world standard for molecular graphics systems for several years has been a laboratory minicomputer and a color line drawing display. This configuration has displaced the earlier line drawing terminal because it offers real-time global viewing of macromolecules and van der Waals surfaces. In attempting to do docking and real-time energy minimization it became clear that there were inadequacies in the present standard configuration. Design and implementation of a new molecular graphics system has begun at the NIH with a goal of eliminating all the known limitations and providing superior graphical and computational capabilities. The technology has improved so that instead of all users sharing one graphics display each user can solve problems at a workstation which includes both a strong computer and good graphics. Users who may be in different buildings are connected to each other and shared devices by a high-speed network. To the network are attached an array processor for real-time energy calculations, a polygon processor for the generation of general surface shapes, and a device called "Joystring" for true six degree of freedom graphical input. For particularly difficult molecular structure problems a special purpose LISP machine will, using artificial intelligence techniques, plan problem solutions by searching and conducting conformational experiments. The general surface drawing capability will be used in representing the structure of cellular and sub-cellular organizations. This paper will be very projective in an attempt to focus interest on problems which might be solved with this new level of equipment.

T-AM-SymII-2 INTERACTIVE REAL-TIME THREE-DIMENSIONAL COMPUTER GRAPHICS Robert Langridge, Computer Graphics Laboratory, University of California, San Francisco, CA (on leave at Department of Computer Science, Stanford University, Stanford, CA)

The problem faced in highly interactive real-time molecular graphics systems is reviewed. Recent work on real-time surface generation and the energetics of molecular interactions is reported.

The critical problem of the user interface is discussed together with possible future applications of artificial intelligence.

Supported by NIH RR1081 and a Guggenheim Fellowship.

T-AM-SymII-3 3-D ANALYSIS AND DISPLAY OF MOLECULES AND NERVES. Cyrus Levinthal, Department of Biological Sciences, Columbia University, New York, NY 10027.

The use of computer graphics for the display and the visual analysis of molecular structures and the anatomy of nerves and nerve nets is well established. However, both for molecules and nerves improved computational ability is needed to make these analyses more useful. Such developments should permit the search of many conformations to select a structure with a global energy minimum and should allow more extensive molecular dynamics calculations than is now possible. In addition, automatic tracing and pattern recognition is needed to reduce the effort required to input anatomical data from successive serial section photographs.

A brief description will be given of a special purpose digital processor, called FASTRUN, currently being designed and constructed as a giant project with the Brookhaven National Laboratories. This device is expected to provide speeds for molecular calculations which would be somewhat greater than that available on a CRAY-1 and at a very much lower cost.

Automatic nerve tracing has been developed in our laboratory with digitized images from aligned 35 mm filmstrips. A very simple isodensity following algorithm then identify the boundaries of many cells and fibers and thus establish the 3-D surface of individual neurons (Sobel, et al., Ann. Rev. Biophys. Bioeng. 9: 347-362). Currently, more sophisticated pattern recognition algorithms have been implemented to deal with those cases in which contour following fail to provide the position of cell or fiber membranes either because of gaps in electron micrographs of membranes or excessively close contact between different cells or between cell membranes and internal organelles. The specifics of the algorithms used and their success with both vertebrate and invertebrate neural tissue will be discussed. This work was supported by NIH grant RR00442.

T-AM-SymII-4 METHODS FOR THREE-DIMENSIONAL DISPLAY AND ANALYSIS OF BIOLOGICAL STRUCTURE
BY Philip J. Mercurio, Mark R. Heckman, Lu-Xi Xu, H.-S. Su, K.-Y. Lau, K.K.L. Ho, Linda Brier, Jeffrey A. Loomis, Michael L. Rhodes, William V. Glenn, Jr., and Robert B. Livingston. Laboratory for Quantitative Morphology, UCSD, La Jolla, CA 92093; Institute of Basic Medical Sciences, Beijing Medical College, Beijing; and Multi-Planar Diagnostic Imaging, Inc., Torrance CA 90505.

We are developing methods for 3-D display and analysis of neuroanatomical material. We seek to compared 3-D structures in different human brains, successive stages of human brain development, and brains of related species. Contour data are acquired by hand tracing individual stained sections or photographs of surfaces of anatomical blocks cut at defined intervals. Data from C-T scans can be derived automatically by a program that produces contours from raster images. Thus, comparisons can be made with living anatomy, normal and pathological.

Contours are maintained as closely as possible in registration and can be re-aligned interactively using computer graphic displays and software. Other programs can create 3-D objects from aligned contours, measure surface areas and volumes, locate centers of gravity, and define the spines of irregular objects. The center of gravity is useful for centering rotation of irregularly-shaped objects. Multiple objects can be arranged in scenes and moved dynamically for motion picture production. Applications of these methods will be shown.

T-AM-SymII-5 THREE DIMENSIONAL STRUCTURE WITHIN CELLS. John W. Sedat. University of California, Department of Biochemistry, San Francisco, CA.

Three dimensional reconstruction of interphase nuclei and chromosomes reveals a heirarchy of nuclear organization. Nuclei within cells are stained with an enhanced lifetime-nonintercalative-DNA specific dye. Images are collected on a eucentric stage fluorescent microscope. Multiple angle and multiple focal plane images are digitized by computer controlled television scanner. Extensive computer graphic analysis is used for image processing, model building, and quantitation of pathway parameters. This scheme entails cubic arrays of processed pixels displayed on a high resolution color raster graphic system.

T-AM-A1 EFFECT OF MEMBRANE POTENTIAL ON INTRACELLULAR pH IN HEART MUSCLE. R.D. Vaughan-Jones, M.B. Cannell and W.J. Lederer. Dept. Physiology, Oxford University, Oxford OX1 3PT, England, and Dept. Physiology, Univ. Maryland, Baltimore, MD21201.

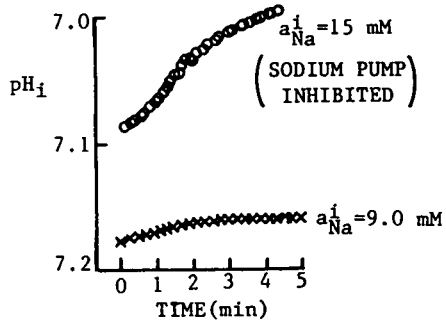

The regulation of intracellular pH (pH_i) is critical to the proper regulation of many cellular functions. We have examined the effect of membrane potential on pH_i in sheep cardiac Purkinje fibres. Membrane potential was controlled using a two microelectrode voltage-clamp while both intracellular sodium activity (a^i_{Na}) and pH_i were measured using ion-sensitive microelectrodes. Fig. 1 compares the effect of a prolonged depolarisation from -70 mV to -30 mV on the time course of pH_i change under two different conditions. When a^i_{Na} was 9.0 mM the 40 mV depolarisation produced only a small effect on pH_i. However, when a^i_{Na} was 15 mM, the same depolarisation produced a significant intracellular acidification of approximately 0.1 pH units. Such voltage-dependent acidifications are accompanied by a decrease in dNa_i/dt and might be explained by an electrogenic Na:H exchange mechanism. However, alternative explanations arise from the observation that when sodium is elevated the depolarisation leads to an increase in Ca^{++}_i (as inferred from the increase in resting tension). This increase in Ca^{++}_i could then result in a displacement of protons from common buffers and/or increased metabolic load from the concomitant contraction, thereby explaining the acidification. Supported by the NIH, American Heart Assoc.& MRC.

T-AM-A2 PHOTOCHEMICAL UNBLOCKING OF Ca^{2+}-ANTAGONISTS IN MAMMALIAN HEART. K.J.Malloy & M.Morad, Dept. of Physiol., Univ. of Penna, Phila., PA

It has been recently shown that Ca^{2+}-antagonists (nifedipine and nisoldipine) may be rapidly photo-inactivated in frog ventricular muscle such that the recovery of tension and I_{si} is complete within one beat (Morad et al., Nature 304:635-638, 1983). We studied the effect of rapid photo-inactivation of nifedipine on cat ventricular trabeculae placed in a single sucrose gap voltage clamp set-up. Following drug equilibration, the first beat after the light pulse (300-400 nm) was accompanied by an action potential (AP) with elevated plateau (10-20 mV) and a duration 2-3 fold over that seen in the presence of the drug. Subsequent beats showed a step-wise decline in plateau height and shortening of AP, reaching a steady-state in 6-8 beats. Tension also recovered slowly. The first post-flash beat was slightly increased, with subsequent beats growing 5-6 fold over that in the presence of drug. Under voltage clamp conditions the first post-flash clamp elicited a marked increase in I_{si} but only a small increase in twitch tension. Subsequent clamps caused a progressive increase in tension, but a concommitant decline in I_{si}. Early (30 msec) and late (700 msec) I-V relations were shifted in the inward direction throughout the test voltage range after the light pulse. The tension-voltage relation was unaltered in shape but increased in magnitude after the drug inactivation. Addition of Co^{2+} (2 mM) to nifedipine-treated muscles prevented tension or I_{si} recovery after the light pulse. The kinetics of redevelopment of I_{si} and tension contrasted sharply with those of the frog heart. Our results suggest that I_{si} is by itself insufficient to fully restore tension; rather it serves to trigger the release of internal Ca^{2+} pools which in turn activates an outward current that shortens and reduces the plateau of the AP.

T-AM-A3 CHANNEL CURRENTS DURING SPONTANEOUS ACTION POTENTIALS IN EMBRYONIC CHICK HEART CELLS. R. Fischmeister, L. J. DeFelice, R. K. Ayer, Jr., R. Levi and R. L. DeHaan. Department of Anatomy, Emory University, Atlanta, Georgia 30322

Single-channel currents were recorded with the cell-attached patch-clamp technique from small clusters (2-20 cells) of spontaneously beating 7-day embryo ventricle cells. Since the preparation was rhythmically active, the membrane potential (Vm) was the whole-cell action potential (AP). The total current through the patch membrane is referred to as the patch action current (AC). After ACs were recorded, the membrane patch was disrupted to record Vm. In some preparations, we sealed patch electrodes to two cells in the same electrically coupled cluster. One electrode covered an intact patch and recorded the patch AC, while the other recorded Vm through a disrupted patch. During normal cell firing the ACs showed individual events superimposed on a background waveform similar in shape to the AP. The amplitudes and shapes of the ACs depended on the number and types of channels in the patch. Only a small fraction of the AC amplitude resulted from the background leak that remained when the channels were closed. The patch I-V relation was constructed by plotting the AC against the AP. When the patch electrode was filled with an intracellular-like, high-K solution, the most common current was an inward rectifier with a reversal potential near -15 mV. With different pipet solutions, other types of channels were seen more often. When the patch pipet contained bath solution, the normal contribution of different specific channel currents to the AP could be recorded directly. (Supported by NIH HL27385).

T-AM-A4 ACTIVATION-DEPENDENT INFLUX AND EFFLUX OF CALCIUM MEASURED WITH EXTRACELLULAR CALCIUM-SENSITIVE DYES IN MAMMALIAN HEART VENTRICLE. D.W. Hilgemann and G.A. Langer, Cardiovascular Research Laboratory, UCLA School of Medicine, Los Angeles, CA 90024

Tetramethylmurexide (TMM) and antipyrylazo III (APIII) were applied extracellularly in isolated mammalian ventricle preparations to attempt to monitor transsarcolemmal calcium (Ca) movements via multiple-wavelength spectrophotometry. Under appropriate conditions extracellular Ca concentration fluctuations can be clearly differentiated from effects of motion on transmitted light. Similar signals are obtained with both dyes. TMM (2 mM) is used with 0.4 to 1.0 mM total Ca (0.2 to 0.5 mM free Ca); APIII (0.6 mM + 5 mM Mg) is used with 0.2 to 0.4 mM total Ca (0.15 to 0.3 mM free Ca). In arterially perfused right ventricle of rabbit, 4 to 8 beats at 2 Hz after a 10 min rest period result in the cumulative depletion of 5 to 15% of total dye-accessible Ca from the extracellular space. During rest or continuous stimulation, extracellular Ca returns toward control levels in 2 to 4 min. Cumulative Ca depletion responses are strongly inhibited by nifedipine (1 μM), but are insensitive to verapamil even when responses take several beats to develop. Isoproterenol (0.1 μM) increases the magnitude of net Ca influx at a single rested state beat to that of the multi-beat response. Ca influx at such a beat appears essentially linear over 300 ms. Under control conditions, a single beat, placed 2 to 30 s subsequent to rapid pacing, results in a net increment of 2 to 5% of total dye-accessible Ca; net Ca efflux is complete by the end of the motion artifact and depletion responses can be demonstrated immediately thereafter. Net influx of Ca corresponds to build-up of a potentiated contractile state; net Ca efflux to its dissipation. The postulate of a voltage-dependent Ca pore in couplings of junctional SR to the sarcolemma may explain turnover to the extracellular space of most of the "activator" Ca pool at a single beat in rabbit ventricle.

T-AM-A5 Na^+ CURRENTS IN SINGLE BULLFROG ATRIAL MYOCYTES. R.B. Clark and W. Giles, University of Texas Medical Branch, Galveston, Texas 77550 and University of Calgary School of Medicine, Calgary, Canada T2N 4N1.

The "gigaohm seal" technique of Hamill et al (Pflugers Arch. 391: 85) was used to voltage-clamp single enzymatically-dispersed myocytes from adult bullfrog (Rana catesbeiana) atrium. Recordings were made at fixed temperatures between 5-12°C and Ca^{++} current was suppressed by 0.1-0.5 mM Cd^{++}. Peak transient inward currents were in the range 0.9-1.6 nA at membrane potentials of -10 to -15 mV for cells held at -80 to -90 mV. The current was half-inactivated at -70±2 mV (n=4), and the apparent reversal potential in 115 mM Na^+ was about +55 mV. The amplitudes of repolarization "tail" currents following depolarizing steps of different durations closely paralleled the time course of i_{Na} (see Fig.). TTX (1 μgm/ml) completely blocked both the activation and deactivation phases of i_{Na}.

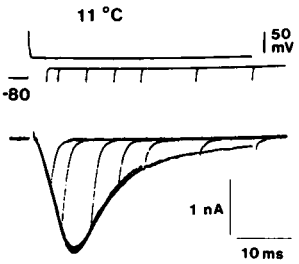

A two-pulse protocol was used to measure rates of inactivation and recovery of i_{Na} in the potential range -50 to -80 mV. Half times for onset of inactivation (t_i) and recovery from inactivation (t_r) differed by less than a factor of 2, e.g., t_i = 0.53 s and t_r = 0.50 s at -60 mV and t_i = 0.64 s and t_r = 0.35 s at -70 mV (T = 11°C). These results are in contrast to previous studies of inactivation and recovery of Na^+ current in frog atrium (Haas et al, Pflugers Arch. 323: 141). Supported by DHHS HL-27454, AHA 81-835, and the Alberta Heritage Foundation.

T-AM-A6 THE EFFECTS OF THE INWARD RECTIFIER ON TRANSMEMBRANE IMPEDANCE PROPERTIES OF ISOLATED MAMMALIAN CARDIAC CELLS. L. E. Moore and G. Isenberg. Department of Physiology and Biophysics, University of Texas Medical Branch, Galveston, Texas, and II Physiological Institute, University of Saarland, Homburg, Germany.

Voltage clamp admittance experiments have shown that single mammalian ventricular cells possess an internal membrane system which has a total membrane capacitance of 4-6 times that of the surface membrane. Based on morphology alone, the most likely structure for the internal membrane capacitance is the sarcoplasmic reticulum rather than the transverse tubular system. In order to test this hypothesis the impedance was measured in hypertonic solutions in which the tubules were swollen. If the series resistance to the inner membrane system is principly determined by dimensions of the tubular structure, then swollen tubules should lead to a decreased value. In fact, the opposite result was found, supporting the hypothesis that the series resistance to the inner membrane system is not the T-tubule lumen. The most likely source of the series resistance is the dyadic junction between the sarcoplasmic reticulum and both the surface and tubular membrane regions. The increase in series resistance caused by hypertonic solutions was proportional to the tonicity and generally reversible. These measurements were done in zero potassium and 20 mM cesium chloride Tyrode's solution in order to block the inward rectifier and measure only the passive electrical circuit. Additional experiments in normal Tyrode's, allowed a determination of the kinetic behavior of the inward rectifier. This analysis is analogous to the usual procedures used in voltage clamp studies to separate ionic currents and leakage conductances. The method of analysis consisted of fitting the real part of the cesium sensitive admittance to Lorentzian functions. This procedure gave an activation time constant for the Cs sensitive inward rectifier of about 1 msec.

T-AM-A7 CARDIAC PACEMAKER CELLS FROM BULLFROG SINUS VENOSUS LACK AN INWARDLY RECTIFYING BACKGROUND K^+ CURRENT. E.F. Shibata and W. Giles, University of Texas Medical Branch, Galveston, Texas 77550 and University of Calgary Medical School, Calgary, Canada T2N 4N1.

A single microelectrode voltage clamp technique (Hume & Giles, J. Gen. Physiol. 81: 153, 1983) was used to record background, or time-independent, current from single, enzymatically isolated cardiac pacemaker cells obtained from the bullfrog sinus venosus. The I-V relation of this current was nearly linear between -140 and +30 mV, with a slope resistance of approximately 2 Gigohms. The reversal potential was near -80 mV in 2.5 mM K^+ Ringers; suggesting that K^+ ions are the major current carriers. $BaCl_2(10^{-5}M)$ failed to produce any significant inhibition of this current.

In contrast, single atrial myocytes obtained from the same heart exhibited a significant inwardly rectifying current, i_{K_1}, which was blocked by $BaCl_2(10^{-5}M)$. These findings, and additional detailed comparisons of the transmembrane currents in sinus venosus and atrial myocytes have identified the major differences between bullfrog sinus venosus and atrial cells. The single pacemaker cells; (1) have no TTX-sensitive Na^+ current, and (2) have no i_{K_1} background current. Sakmann et al. (Nature, 303: 250-253, 1983) have previously reported that mammalian S-A node cells also lack conventional inwardly rectifying background K^+ current. The absence of i_{K_1} may explain the relatively positive "resting" potential in quiescent sinus pacemaker cells, and their relative insensitivity to changes in $(K^+)_o$.

Supported by DHHS-HL-27454, AHA 81-835, the Canadian MRC, and The Alberta Heritage Foundation.

T-AM-A8 AN ELECTROGENIC Na^+/K^+ PUMP CURRENT IN INDIVIDUAL BULLFROG ATRIAL MYOCYTES. E.F. Snibata, Y. Momose and W. Giles. (Intr. by R.D. Baker). Department of Physiology and Biophysics, University of Texas Medical Branch, Galveston, Texas 77550 and the University of Calgary Medical School, Calgary, Canada T2N 4N1.

Recent electrophysiological data strongly suggest that in a variety of multicellular cardiac muscle preparations, the Na^+/K^+ pump operates in an electrogenic mode. We have tested this possibility in enzymatically dispersed cells from bullfrog atrium, using a whole-cell, single microelectrode voltage clamp technique. Suspensions of cells were Na^+ loaded during a 20 minute incubation in 0 mM KCl Ringers solution. $BaCl_2$ (0.5 mM) was included to inhibit the inwardly rectifying background potassium current. Following re-addition of K^+ (2.5 mM) or Rb^+ (20 mM) a transient outward current, approximately 55 ± 7 pA (n = 7) at peak, was recorded (see Fig.).

This current is inhibited 80-90% by strophanthidin (10^{-5} M); it is therefore thought to be due to activation of an electrogenic Na^+/K^+ pump. From the available data on:

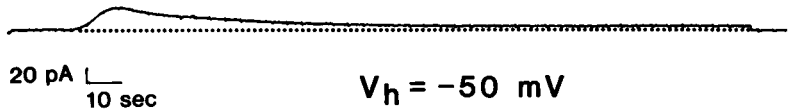

(1) cell surface area ($4x10^3$ μm^2/cell), (2) coupling ratio ($3Na^+/2K^+$), (3) pump site density (e.g. 500/μm^2), and (4) turn-over rate (e.g., 100/sec), an electrogenic current of 33 pA/cell is predicted. Supported by DHHS HL-27454, AHA 81-835, and the Alberta Heritage Foundation.

T-AM-A9 ACTIVATION OF THE INWARDLY RECTIFYING K^+ CURRENT IN GUINEA PIG ISOLATED ATRIAL AND VENTRICULAR CELLS. Y.Tourneur, R.Mitra & M.Morad. Univ. of Penna., Dept. of Physiol., Philadelphia, PA.

The inwardly rectifying K^+ current has been identified in a variety of conventional myocardial preparations as a quasi-instantaneous system. In isolated heart cells, even the existence of an outward current and a negative slope has been questioned. We studied this current in enzymatically isolated (collagenase, protease) adult myocytes using a suction pipette voltage clamp technique. Seal resistances ranged between 1-15 giga ohms in 5 mM Ca^{2+} Tyrode's. I_{si} was blocked by 3 mM Co^{2+} and 1 uM Diltiazem. I_{Na} was inactivated by a depolarizing prepulse. Fig. 1 shows a negative slope conductance for positive steps and time-dependence for negative steps. Similar kinetics were observed in solutions without Na^+, Ca^{2+} or Cl^- as well as in isotonic potassium solutions. The time dependent inward and steady state current was reversibly blocked by 5 mM Cs^+ or 500 uM Ba^{2+}.

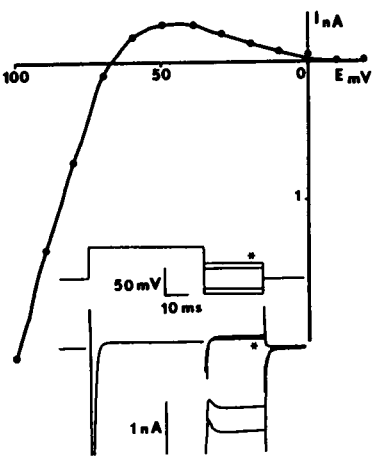

Our experiments show that in isolated heart cells, the inwardly rectifying K^+ current has a similar I-V curve, time, and ionic dependence as that described for intact cardiac tissue and the inwardly rectifying K^+ current of skeletal muscle and starfish eggs.

T-AM-A10 DELAYED RECTIFICATION IN THE CALF CARDIAC PURKINJE FIBER: EVIDENCE FOR K^+ SELECTIVITY AND MULTIPLE STATE KINETICS. P.B. Bennett, L.C. McKinney, R.S. Kass and T. Begenisich, Department of Physiology, University of Rochester, Rochester, NY 14642.

We have investigated the delayed rectifier (I_x) in the calf cardiac Purkinje fiber using a conventional two-microelectrode voltage clamp arrangement and have addressed several open questions about this current. The deactivation of I_x was monitored by studying decaying outward current tails after the application of depolarizing voltage prepulses. The reversal potential of these I_x tails (E_x) was measured as a function of prepulse magnitude and duration to test for possible accumulation-induced changes in K^+_o. We found that prepulse-induced changes in E_x were $\leq$ 5 mV (N=9) provided that prepulse durations were $\leq$ 3.5 sec and magnitudes were $\leq$ +60 mV. We kept voltage pulse structure within these limits for the remainder of the experiments in this study. Under these conditions, we studied the sensitivity of E_x to variation in extracellular K^+. The equilibrium potential for I_x is well-described by a Goldman-Hodgkin-Katz relation for a channel permeable to Na^+ and K^+ with P_{Na}/P_K=.04. We then studied I_x kinetics. We measured the voltage-dependence of the I_x time constants and determined that steady-state activation curves could be measured within the limits established by the loading experiments. The deactivation of I_x was always found to be biexponential under the conditions in these experiments, and the two components of this current share a common equilibrium potential. This result suggests that it is not necessary to postulate the existence of two populations of channels to account for the time course of the I_x tails. Instead we interpret these data as providing evidence that I_x channels are a single population that can exist in more than two states.

T-AM-A11 OPTICAL MEASUREMENTS OF EXTRACELLULAR CALCIUM DEPLETION IN FROG VENTRICULAR STRIPS. L.Cleemann & M.Morad. Dept. of Physiol., U. of P., Phila., PA & M.D.I.B.L., Salsbury Cove, ME.

Frog ventricular muscle is examined in a single sucrose gap voltage clamp set-up equipped for simultaneous measurements of transmission of light through the strip at 3 different wavelengths. With antipyrylazo III added to the perfusate the Ca-induced signal was measured at 724 nm while contraction artifacts are measured at the isosbestic point (620 nm) and at 788 nm where the dye is transparent. Motion artifacts were reduced by: stretching the strip, gently squeezing it between the moveable transparent walls of the chamber, and by subtracting a weighted average of the motion artifacts measured at the two other wavelengths. The Ca-depletion signal measured during individual beats has the same wavelength dependency as the Ca-induced difference spectrum of the perfusate. The time course of the Ca depletion was unchanged when the concentration of antipyrylazo was varied (2 or 0.2 mM), when tetramethylmurexide was used as an extracellular Ca probe instead of antipyrylazo, or when tension was suppressed by hypertonic solution. Comparison of the Ca-depletion signal with the twitch force shows that the rate of Ca depletion is maximal immediately after the upstroke of the action potential, i.e. before any force development occurs, and that Ca-depletion has its maximal value (0.01 to 0.2 mM) at the end of the action potential but shortly before the peak of the twitch. Epinephrine enhanced tension and the Ca depletion signal. A clamp pulse which prematurely terminated the action potential also shortened the Ca depletion signal. These results show that optical techniques can be used to study rapid changes in the extracellular Ca content and suggest that this method may be used to study the voltage- and time-dependence of sarcolemmal Ca influx.

T-AM-B1 OUTWARD SODIUM FLUXES ACROSS THE CELLULAR PATHWAY IN TIGHT EPITHELIA.
Howard F. Schoen and David Erlij (Intro. by Eleanor B. McGowan). S.U.N.Y., Downstate Med. Ctr., Brooklyn, N. Y. 11203

We have examined in the isolated frog skin intracellular potential and the movements of Na^+ under conditions of reversed Na^+ electrochemical gradient to obtain information on two points: a) the movements of Na^+ across the basolateral membrane, and b) whether a net efflux of Na^+ across the apical membrane can be demonstrated. We measured current and Na^+ fluxes in skins clamped at a transepithelial potential of 0 mV and with an apical-side solution which was nominally Na^+-free ([Na^+] less than 35 μM). Under these conditions more than 80% of the skins generated an outward- (basolateral to apical) directed current that ranged between 0.5 and 3.5 $\mu A/cm^2$. This current was abolished by amiloride. The outward amiloride-sensitive current was markedly increased when either oxytocin or ouabain was added to the basolateral solution. The amiloride-sensitive outward Na^+ flux and current are in close agreement. Measurement of intracellular potential showed that addition of amiloride under conditions of net outward Na^+ flux caused a depolarization of the intracellular potential, the opposite of what is seen under conditions of inward Na^+ transport. This indicates that some, if not all, of the outward Na^+ flux occurs across the cellular pathway. We conclude that: a) there can be an important Na^+ flux across the basolateral membrane, and b) inversion of the electrochemical gradient for Na^+ across the apical barrier reverses the direction of Na^+ flux.
(Supported by the N.I.H. and the New York Heart Association.)

T-AM-B2 TRANSIENT VOLTAGE RESPONSE OF THE ISOLATED FROG SKIN TO BRIEF CONSTANT CURRENT PULSES IN THE PRESENCE AND ABSENCE OF AMILORIDE. J.T. Tarvin and M.A.Dinno, Department of Physics and Astronomy, University of Mississippi, University, MS 38677

Abdominal skin patches of Rana pipiens, symmetrically bathed with amphibian Ringer, were subjected to 0.5 second duration transmembrane pulses of constant current (4.0 to 12.5 μA per 0.84 cm^2). The resulting transmembrane potential was digitized every 50 μs for a total of 1024 data points. Least-squares analysis of this data for a single exponential function plus a linear background term yielded a time constant given by RC = 4.1 ± 0.4 ms where R = 1032 ± 56 ohm-cm^2 and C = 4.0 ± 0.4 $\mu f/cm^2$ (mean ± SE, N = 6). These findings are similar to those of Smith (Smith, P.G. Acta physiol. scand. 81:355-366, 1971) who, using an AC method, found that frog skin bathed in NaCl Ringer could be represented by a single parallel RC circuit which was associated with the outer, pond-facing membrane. Our present findings agree with this interpretation, since the addition of amiloride (2.5 μM) to the outer membrane bathing solution resulted in increases of R and RC by factors of 1.30 ± 0.07 and 1.29 ± 0.07 (mean ± SE, N = 6), respectively, with no significant effect on capacitance. These findings are consistent with the known mechanism of action of amiloride in that its effect is on the Na channel conductance and not on the membrane area. A possible identification of the contribution of the inner membrane to the voltage transient will be discussed. Supported by ONR Contract No. N00014-81-K0663 and University of Mississippi Faculty Research Grant.

T-AM-B3 A BALANCED GRADIENT MECHANISM FOR ISOTONIC WATER TRANSPORT. Richard T. Mathias; Rush Medical College; Chicago, Illinois, 60612.

The relationship between epithelial fluid transport, standing osmotic gradients and standing hydrostatic pressure gradients has been investigated using a perturbation expansion of the governing equations. The assumptions used in the expansion are: (1) the volume of lateral intercellular space (LIS) per unit epithelial volume is small; and (2) owing to a large membrane hydraulic conductivity, the length constant for fluid movement along the LIS is much shorter than the thickness of the epithelium. In this circumstance, there needs to be substantial hydrostatic pressure gradients along the LIS to move the fluid longitudinally. The positive hydrostatic pressure within lateral spaces tends to drive transmembrane water flow back into cells, but this tendency is countered by osmotic gradients within the LIS, which balance (to some 99%) hydrostatic pressure. Furthermore, the positive hydrostatic pressure within the LIS tends to drive fluid out the apical as well as basal end of the space. The overall pattern of flow is: water moves into cells across apical and basal membranes; water moves out of cells into the LIS; water flows out of apical and basal ends of the LIS. Net absorption is conferred by a relatively large area of apical membrane and the presence of junctions at the apical end of the LIS. There must also be a small, unbalanced osmotic gradient which pulls fluid into the lateral space and drives the entire system. This analysis neglects electrical forces but the abstract by McLaughlin and Mathias, 1984, of this session, extends these results to include voltage.

Supported by NIH grants EY03095 and HL29205.

T-AM-B4 THE ROLE OF ELECTRO-OSMOSIS IN THE REABSORPTION OF FLUID FROM THE RENAL PROXIMAL TUBULE. Stuart McLaughlin and Richard Mathias. HSC, SUNY Stony Brook, NY 11794 and Rush Medical College, Chicago, IL 60612.

We postulate that electrogenic sodium pumps in the basolateral membranes produce an electrical potential within the lateral intercellular space (LIS), that the lateral membranes bear a net negative charge, and that fluid moves parallel to these membranes because of Helmholtz-type electro-osmosis, the field induced movement of fluid adjacent to a charged surface. Our theoretical analysis indicates that the sodium pumps should produce a longitudinal electric field of order 1 V/cm in the LIS. Our experimental measurements on rat renal basolateral membrane vesicles demonstrate that the electrophoretic mobility of the vesicles, which is also the electro-osmotic fluid velocity in the LIS produced by a unit electric field, is 1 μm/s per V/cm. Thus, our model predicts that the fluid velocity in the LIS due to electro-osmosis is of order 1 μm/s, which is sufficient to account for the observed fluid flow in renal proximal tubules. Several experimentally testable predictions emerge from our model. First, the pressure in the LIS is predicted to be negative (subatmospheric). In agreement with this prediction, the LIS of rabbit proximal tubules appear not to swell during fluid transport (Burg and Grantham, 1971). Second, a voltage clamp of -15 mV (lumen negative) should cause fluid to be secreted in the Necturus proximal tubule, a prediction that agrees quantitatively with the experimental observations of Spring (1973). Third, any substance that reverses the charge on the basolateral membranes (e.g. thorium) should cause the LIS to swell.

Supported by NIH grants GM24971 (S McL), EY03095 (R M), & HL29205 (R M) and NSF grant PCM8340253.

T-AM-B5 MICROELECTRODE ARTIFACT AND THE DONNAN POTENTIAL. W. S. Rehm, M. Schwartz, G. Carrasquer Department of Medicine (Nephrology) and Physics, University of Louisville

In three tissues (stroma of frog cornea, frog striated muscle with plasma membrane removed, connective tissue of frog skin), a 3 M KCl microelectrode (m.e.) is negative to an external electrode. Some call this a Donnan potential. In our work on frog stroma, we interpret the PD as due to effect of fixed negative charges of connective tissue fibers on the ratio (R) of K^+ to Cl^- mobilities. The average PD in the stroma with 3 M KCl, 1 M KCl, or Ringers in the m.e. is respectively 23 mV, 15 mV and zero. With stroma mounted between chambers and with Ringers on one side and 3 M KCl on other side, the PD with macroelectrodes in bathing solutions is zero which seems incompatible with the above. However, when the 3 M KCl m.e. first contacts the stroma, bathed in Ringers, the PD is zero. Stepwise advancement of the m.e. increases stepwise the negativity of m.e. If fibers have a Debye length of 1 nm and distance between fibers $\gg$ 1 mm, overall $R \simeq 1$. Stepwise advancement of m.e. distorts geometry (decreasing distance between fibers at m.e. tip) and R becomes >1. Hence a 3 M KCl m.e. becomes more negative. Since the PD is a function of $[KCl]$, in m.e. the PD is not a Donnan potential. Distorted fiber geometry makes an analytical solution of PD vs. $[KCl]$ extremely difficult. Even with a simple geometry (i.e., a rectangular pore spanning the membrane with the long sides charged) solution of the 2 dimensional Poisson-Boltzmann equation is difficult and more so with asymmetrical media. For simplicity the potentials in certain domains of such systems have been called Donnan potentials. However, the PD with 3 M KCl m.e. is a diffusion and not a Donnan potential. NSF and NIH support.

T-AM-B6 MUCOSAL IBMX (3-ISOBUTYL-1-METHYL XANTHINE) DECREASES K^+ BASOLATERAL CONDUCTANCE IN GALLBLADDER EPITHELIAL CELLS. W. McD. Armstrong, D.C. Zeldin, and A. Corcia, Dept. of Physiology and Biophysics, Indiana University School of Medicine, Indianapolis, Indiana 46223.

Agents that increase cellular cAMP enhance apical membrane Cl^- and HCO_3^- conductances in epithelia. We found that 3-isobutyl-1-methyl xanthine (IBMX), a known phosphodiesterase inhibitor, increases cAMP levels in Necturus gallbladder. We used conventional microelectrodes to study the effects of IBMX on membrane conductances in gallbladders mounted in a divided chamber and bathed by Ringer's solutions at 23°C and pH 7.4. In HCO_3^- free solutions, 10^{-4} M IBMX added to the mucosal medium depolarized the apical membrane potential, V_a (-59±2 mV, SEM, n=16), by 13±2 mV and decreased the fractional resistance, F_R, by 0.37±0.03. In solutions containing 25 mM HCO_3^-, IBMX caused a transient hyperpolarization of V_a (3±1 mV, n=11) followed by a depolarization that did not differ significantly from that observed in HCO_3^- free Ringer's. Removal of mucosal Cl^-, Na^+ or Ca^{++} did not affect the depolarization in V_a caused by IBMX. The basolateral membrane of Necturus gallbladder is highly K^+ permeable. Increasing serosal K^+ from 2.5 to 80 mM depolarized V_a by 19±2 mV (n=5). Mucosal IBMX reduced this depolarization to 10±3 mV (n=5). Addition of 10 mM Ba^{++} to the serosal medium depolarized V_a by 7±1 mV (n=4). In the presence of serosal Ba^{++}, IBMX depolarized V_a by 2±1 mV (n=4). These results indicate that mucosal IBMX increases apical HCO_3^- conductance and decreases basolateral membrane K^+ conductance in gallbladder epithelial cells via a cAMP-dependent mechanism. Decreased basolateral K^+ conductance appears to be the major determinant of the IBMX-induced depolarization of V_a.

Supported by USPHS AM 12715.

T-AM-B7 INTRACELLULAR CALCIUM ACTIVITY IN SPLIT FROG SKIN EPITHELIUM. Ellie Kelepouris and Mortimer M. Civan. Departments of Medicine and Physiology, University of Pennsylvania School of Medicine, Philadelphia, Pennsylvania 19104.

Cytosolic calcium activity (a^c_{Ca}) is critical in regulating a wide range of cellular functions, including transepithelial transport. Measurement of a^c_{Ca} by ion-selective microelectrodes has previously been technically limited to relatively large cells ($\geq$20μm). We now report results obtained with the small epithelial cells (~10μm) of split frog skin. Borosilicate glass capillaries were pulled to the same configuration as that of our reference micropipets used for basolateral impalements. Reference micropipets were filled with 0.5M KCL. Microelectrodes were prepared by coating with hexamethyldisilazane vapor, heating, filling the tip with resin incorporating neutral Ca^{++} ligand and backfilling with 100 mM $CaCl_2$. A decade change in Ca^{++} concentration produced an electrode response of 30±1 mV (mean ±SE) for Ca^{++} concentrations of 10^{-3} - 10^{-6} M (pCa 3-6) and 26±1 mV for pCa 6-7. The ratio of the microelectrode sensitivity at pCa 6-7 to that at pCa 3-6 was 0.87±0.03, comparing favorably with values previously reported. The outputs of the reference micropipet (ψ^{sc}) and the Ca^{++}-microelectrode (E^{sc}_{Ca}) within the cell relative to the serosal medium were measured simultaneously within the short-circuited epithelium. As previously documented, the syncytial properties of this preparation permit ψ^{sc} and E^{sc}_{Ca} to be measured with single-barrelled micropipets and microelectrodes in separate cells. In 8 successful experiments, short circuit curent was 8.2±0.9 $\mu A \cdot cm^{-2}$, total tissue resistance was 3.3±0.7 $k\Omega \cdot cm^2$, ψ^{sc} was -74±3 mV (uncorrected for junction potential) and E_{Ca} was -167±6 mV. Assuming an extracellular calcium activity coefficient of 0.35, a^c_{Ca} is calculated to be 136±24 nM, in agreement with estimates in other tissues. The ability to monitor intracellular calcium activity with microelectrodes in this preparation will allow, for the first time, direct and simultaneous evaluation of the relationship between this parameter and transepithelial transport.

T-AM-B8 EFFECT OF Ag^+ ON ISOLATED BULLFROG GASTRIC MUCOSA. P.K. Rangachari and Jeffrey Matthews. From the Departments of Surgery and Anatomy, Harvard Medical School and the Department of Surgery, and the Charles A. Dana Research Institute, Beth Israel Hospital, Boston, Massachusetts

In nitrate solutions, Ag^+ added to the luminal side has marked effects on transmucosal conductance and PD. Conductance increased quickly (85% within 60 seconds, 420% by 10 mins.); PD increased initially (11% within 30 seconds) and then fell precipitously (58% decreased within 2 mins, 85% decreased by 10 mins). During this period, no increase in mannitol permeability was found. These changes were essentially similar in histamine-stimulated, spontaneously secreting and metiamide-inhibited fundic mucosae. Similar changes occurred also in the antrum. In $SO_4^=$ media, the increases in conductance occurred more slowly (40% within 2 mins., 150% after 10 mins.); PD increased initially for 4-6 mins. and then slowly declined over 60 mins. to 74% of control values. Replacement of luminal Na^+ by choline had no effect on the changes observed. The increased conductance noted, persisted even after removing Ag^+ and was related to the nature of the anion present in the luminal solution, with the following anion selectivity (NO_3^- > isethionate $\triangleq$ $SO_4^=$ $\triangleq$ acetate > glutamate). Ag^+ appears to alter the anion conductance of the apical and/or junctional membranes.

Supported in part by USPH Grants AM15681 and AM30303

T-AM-B9 SINGLE CHANNEL RECORDINGS OF APICAL MEMBRANE CHLORIDE CONDUCTANCE IN A6 EPITHELIAL CELLS. L.G. Palmer[1], J.M. Tang[2] and D.J. Nelson[2]. [1]Dept. Physiology, Cornell U. Medical College New York, NY and [2]Dept. Physiology, Rush Medical College, Chicago, IL

The apical membrane of epithelial cells from the A6 cell line was studied using the patch clamp technique. In about 50% of the patches, channels with conductances of 360 ± 45 pS in symmetrical 105 mM NaCl solutions were observed. Using excised membrane patches with a 5:1 NaCl gradient across the membrane, the reversal potential was 29-30 mV, indicating a permeability ratio $P_{Cl}:P_{Na}$ of about 9:1, calculated from the constant field equation. Selectivity for Cl over SO4 was weak; $P_{Cl}:P_{SO4}$ was about 2:1, measured from the reversal potential under biionic conditions. The channel was most active at membrane potentials between ± 20 mV and inactivated, usually within a few seconds, at higher potentials of either polarity. Reactivation from this inactivation was slow, sometimes requiring minutes. In addition to the fully active state a flickering state, which appeared to involve rapid transitions to one or more submaximal conductance levels, was observed. The disulfonic stilbene SITS inhibited the conductance in a manner characteristic of reversible open-channel blockers. The channel could mediate transepithelial Cl reabsorption under conditions where the apical membrane voltage difference is small. Supported by NS 18587, AM 27847 and the Whitaker Foundation.

T-AM-C1 EXTERNAL POTASSIUM IONS ALTER K CHANNEL KINETICS IN SQUID AXON. H.M. Fishman, D. Poussart and H.R. Leuchtag. Dept. of Physiology & Biophysics, University of Texas at Galveston, Dept. de Genie Electrique, Universite Laval, Quebec, and Dept. of Biology, Texas Southern University, Houston.

K channel kinetics for inward K currents were compared with those for outward K currents in squid axons with axial electrodes and step voltage clamps from a holding potential of -70mV. Outward currents in 295mM K_i/ASW+1μM TTX were activated by step depolarizations and "drooped" in a characteristic manner during 80 msec duration steps. In high external K (440mM K-ASW+TTX), $E_K>0$, and upon depolarization from -70mV the net current flows inwardly instead of outwardly. The inward currents were transients that activated more slowly (ca.2X) and decayed, due to a concurrent decrease of K conductance, for steps up to 0mV from holding. For steps to >0mV, the decaying phase of the inward current transient disappeared. The tail currents required at least two exponentials for fitting, even for voltage steps to >0mV. The inward K currents were suppressed by 10mM 4-AP added to the K-ASW+TTX or 50mM TEA added to the perfusate. Thus, TEA inhibits K currents, regardless of the direction of the current, whenever it is driven into the membrane by the electric field. The altered kinetics of the channel cannot be attributed to K depletion of the periaxonal space because of the high external K. Because these modifications of K channel kinetics are not apparent in outward currents, it appears that the potassium effects occur in a region outside the K channel, which is accessible only from the external medium.

Supported by NIH grant NS11764 and CRC grant A-5274.

T-AM-C2 EVIDENCE THAT SQUID K CHANNELS CONTAIN A CALCIUM ION WHEN CLOSED. C. M. Armstrong and D.R. Matteson, Department of Physiology, University of Pennsylvania, Philadelphia, PA 19104

The properties of voltage activated K channels were studied in internally perfused, voltage clamped squid giant axons as external calcium concentration (Ca) was varied. Increasing Ca from 20 to 100 mM (20 Ca 501 Na vs 100 Ca 338 Na, with TTX in all solutions) slows channel opening, and is kinetically equivalent to decreasing the depolarizing step by about 25 mV. The same Ca increase shifts the conductance-voltage curve, equivalent to decreasing the depolarizing step by about 10 mV. The effect of a Ca increase on closing kinetics depends on whether K channel-permeant monovalent cations are present in the bath. If not, Ca has a negligible effect on closing. Addition of K, Rb, or NH_4 to the bath slows closing kinetics and makes them more complex. Particularly in Rb, closing kinetics have pronounced slow components. Ca antagonizes the effects of monovalents on closing kinetics. Thus increasing Ca speeds closing only if it has been slowed by K, Rb, or NH_4. The results are not compatible with classical surface charge theory, which postulates the accumulation or binding of Ca near a diffuse layer of negative charge, and equal shifts of all gating parameters. We propose 1) that opening kinetics are slowed by binding of Ca to negatively charged parts of the gating apparatus that are at the external surface of the channel protein when the channel is closed. The negative charge moves inward on activation, removing the impetus for Ca binding. Ca thus has no effect on closing kinetics (unless there are permeant monovalents externally). 2) Ca (or possibly Mg) normally occupies closed channels, and has a latching effect. External K or Rb compete with Ca for channel occupancy. Although the channel can close when occupied by K or Rb, the latching action of Ca is missing and the channel tends to reopen. The tendency to reopen slows final closing.

T-AM-C3 COMPARATIVE EFFECTS OF ANTIFIBRILLATORY AND ANTIARRHYTHMIC COMPOUNDS ON MEMBRANE CURRENTS IN SQUID GIANT AXONS. John R. Clay[1] and Marvin Bacaner[2*,1] Lab. of Biophysics, NINCDS, NIH, MBL, Woods Hole, MA 02543 and [2]Dept. of Physiology, Univ. of Minnesota, Minneapolis, MN 55455.

We have studied the effects of the antifibrillatory compounds bretylium tosylate and bethanidine sulfate on the potassium and sodium currents, I_K and I_{Na}, of squid giant axons using axial wire voltage clamp techniques. Addition of bretylium to our internal perfusate at a concentration of 1 mM reduced peak I_{Na} by 30% and I_K at V=+30 mV by 75% (holding potential = -80 mV); bethanidine (1 mM) reduced peak I_{Na} by 45% and I_K by 70%. The relative difference in the effects of these drugs on I_{Na} was readily apparent at higher concentrations. An internal concentration of 5 mM bretylium reduced peak I_{Na} by 55%, whereas 5 mM bethanidine reduced peak I_{Na} by 85% (Table). We compared these results with the effects of lidocaine and procainamide. These drugs produce an antiarrhythmic effect on the heart and a local anesthetic effect on nerve. Addition of 5 mM lidocaine to the internal perfusate reduced peak I_{Na} by 40% and I_K at +30 mV by 45%. Procainamide produced similar effects (Table). Our results suggest that the antifibrillatory and antiarrhythmic drugs may be categorized by their relative effects on I_K. The antiarrhythmic drugs are weak blockers of I_K, whereas the antifibrillatory compounds are relatively potent blockers of the I_K component.

	Bretylium	Bethanidine	Lidocaine	Procainamide
Antifibrillatory	Primary	Primary	Secondary	None
Antiarrhythmic	Secondary	Secondary	Primary	Primary
Block of I_{Na}	55%	85%	40%	40%
Block of I_K	90%	75%	45%	40%

T-AM-C4 POTASSIUM CHANNELS IN THE NODAL MEMBRANE OF RAT NERVE FIBERS. E. Goren, H. Bergman & Y. Palti. Rappaport Inst. & Dept. of Physiol. & Biophys. Med. Sch., Technion, Haifa, Israel.

Single myelinated nerve fibers from the sciatic nerve of rats were studied in the voltage clamp. Potassium currents were measured in TTX Ringer as a function of nodal membrane area, conditioning and test membrane potentials. In view of Chiu & Ritchie's report (Nature,284,170,1980) that potassium currents seem to appear only after myelin is manipulated & the paranodal areas are exposed (in rabbits), the nodal area was continuously monitored. The functional nodal area was estimated by measuring membrane capacity using the triangular wave voltage clamp (Palti & Al. J. Memb. Biol. 1,431,1969). Furthermore, the nerve chamber was modified such that the nodal area could be visually monitored & photographed so that demyelinization could be directly observed. Delayed potassium currents were demonstrated in intact nodes with relatively stable membrane capacities compatible with those measured in frogs. However, at holding potentials of -60 to -70 mv,practically all channels were already open. This behaviour was compatible with a shift of parameter n on the voltage axis (Bina & Palti, Nature,290,1,1981). The kinetics of the channel closing on hyperpolarization were voltage dependent and much slower then thau n (10-50ms). Upon membrane depolarization (following a conditioning hyperpolarization), there was initially a small rapid transient decrease in current and subsequently an increase with two time constants. The first resembled in all respects "normal" potassium turn-on kinetics, while the second was about ten fold slower. The behaviour of the mammalian potassium channels is compatible with a kinetic model having at least two closed states, an open state and an inactivated state. Supported by N.I.H. grant # 1 R01 NS17127 01A1

T-AM-C5 FAST K CHANNELS OF FROG MYELINATED NERVE APPEAR TO EXIST IN MULTIPLE CONDUCTIVE FORMS. F. Conti, B. Hille and W. Nonner. From the Departments of Physiology and Biophysics of the University of Washington, Seattle, WA 98195, and of the University of Miami, Miami, FL 33101.

Stationary current through K channels of axons has been reported to undergo slow fluctuations whose power spectrum is of the '1/f' type. We find slow fluctuations also when K current is sampled during brief (e.g. 20 msec) depolarizations, separated by 2-5 sec intervals at voltages where K channels are shut. Non-stationary ensemble covariances calculated from such records show short correlations (reflecting the activation kinetics of K current) as well as a long correlation not evident in the time course of the average current. The long-correlation component emerges within msec after the onset of a depolarizing pulse and, in experiments with long (1 sec) pulses, persists during the entire depolarization. Because of its rapid onset, this fluctuation cannot be attributed to gating in a population of very slow K channels. An alternate explanation might be a slow process that varies the number of (fast) K channels available from one trial to the next; one then expects the associated covariance component to follow the time course of the average K current. The experimental covariance, however, develops with a delay longer than that of the average current and, in projections relative to a late time when K current is stationary, starts with a negative phase. This indicates that the slow fluctuation involves interconversions among at least two conductive forms of K channel, rather than among a conductive and a silent form. Experimental covariances are fitted by a model in which a dominant form of K channel activates to a steady conductance near 13 pS and an alternate form activates transiently to a higher conductance (>30 pS) and then inactivates. (Supported by NIH grants NS 08174 and GM 30377).

T-AM-C6 NEURAL CONTROL OF THE ANOMALOUS RECTIFIER CHANNEL IN TONIC MUSCLE FIBERS OF THE FROG. M. Huerta and E. Stefani. Department of Physiology and Biophysics, Centro de Investigación del IPN, Apartado Postal 14-740, México, D.F. 07000, MEXICO.

Tonic fibers do not produce action potentials and do not show anomalous rectification. After denervation, tonic fibers generate propagating Na dependent action potentials. We tested whether the lack of the anomalous rectifier channel is also under neural control. The electrical properties in control and denervated twitch and tonic fibers of the cruralis muscles were measured. Muscle fibers were current clamped with standard two microelectrode technique in the following solution at 20°C (mM/l): KCH_3SO_3 120, and $Ca(CH_3SO_3)_2$ 1.8 (pH 7.4). Normal twitch and tonic fibers were identified according to their passive electrical properties. In both fiber types the resting potential was -7.0±1 mV (7). Tonic fibers have a large effective resistance (V_o/I_o) of 1.7±0.1 MΩ ($\bar{x} \pm$ S.E., n=7), while V_o/I_o in twitch is 0.54±0.04 MΩ (4). The membrane time constant was 44.8±2 msec in tonic fibers and always smaller than 10 msec in twitch fiber. Anomalous rectification was expressed as the ratio of the effective resistance for hyperpolarizing and depolarizing pulses. Normal twitch fibers showed a ratio of 0.45±.1 (14) while tonic fibers had a linear behaviour with a ratio of 1±0.05 (15). After denervation, tonic and twitch fibers can be identified by their passive electrical properties. V_o/I_o in tonic fibers was 1.14±0.3 (5) MΩ while in twitch fibers was 0.43±0.04 MΩ. Denervated tonic fibers showed anomalous rectification, the resistance ratio between hyperpolarizing and depolarizing pulses was 0.48±.07 (5). A similar ratio of 0.45±0.1 (14) was measured in denervated twitch fibers. These results suggested that denervation induce anomalous rectification channels in tonic muscle fibers. Supported by CONACyT (México), grant PCCBNAL-790022.

T-AM-C7 ZINC AND BARIUM INHIBITION OF POTASSIUM EFFLUX THROUGH THE INWARD RECTIFIER IN FROG SKELETAL MUSCLE. B.C. Spalding, J.G. Swift* and P. Horowicz. Dept. of Physiology, Univ. of Rochester, Rochester, NY 14642.

For steady internal potentials (V_i) more positive than -25 mV, K^+ moves through inward rectifier channels. To explore the effects of varying (a) $[K^+]_o$ at constant V_i and (b) V_i at constant $[K^+]_o$ on the inhibition of K^+ efflux by divalent cations in sartorius muscles we have employed solution modifications first introduced by Boyle and Conway. For example, muscles equilibrated in a solution containing 75 mM KCl plus 60 mM NaCl (abbr. 75K/240Na) have the same V_i as when equilibrated in solutions containing 150K/240Na; namely, about -22 mV. In these solutions higher concentrations of Ba^{++} are required to produce a given amount of inhibition when $[K^+]_o$ is increased. The $[Ba^{++}]_o$ which produces 50% inhibition increases from 0.24 mM to 0.78 mM, i.e. by a factor of 3.2, on doubling $[K^+]_o$ from 75 mM to 150 mM. For V_i between -27 mV and -7 mV and $[K^+]_o$ between 75 mM and 300 mM, the main features that emerge are that external K^+ protects against Ba^{++} inhibition at constant V_i and that Ba^{++} inhibition is relatively insensitive to changes in V_i less than 12 mV at constant $[K^+]_o$. Zn^{++} also inhibits K^+ efflux under similar conditions, but raising $[K^+]_o$ does not alter inhibition by Zn^{++}. Lowering the external pH markedly reduces inhibition by Zn^{++} but does not affect inhibition by Ba^{++}. Varying $[K^+]_o$ is also known not to affect inhibition of K^+ efflux by external Rb^+ under similar conditions. Neither lowering external pH nor prior partial inhibition by Zn^{++} significantly affects inhibition by Rb^+. These observations indicate that Zn^{++} inhibition of the inward rectifier is produced by a mechanism different from those involved in inhibition by either Ba^{++} or Rb^+. (Supported by grants from the USPHS and the MDA).

T-AM-C8 EXTERNAL $[K^+]$ AND THE Cs^+ BLOCK OF THE K^+ INWARD RECTIFIER IN FROG SKELETAL MUSCLE. Oksana Senyk (Intr. by Paul Horowicz), Univ. of Rochester, Rochester, NY 14642.

The Hille-Campbell vaseline-gap voltage clamp technique was used to examine the effect of external K^+ concentration on the voltage-dependent block of K^+ currents through the inward rectifier K^+ channel by external Cs^+ in single frog skeletal muscle fibers. The cut ends of the fibers were bathed in 126 mM K-glutamate; 5 mM $MgSO_4$; 1 mM EGTA: 0.5 mM Na_2-ATP; 10 mM HEPES; 1.2 mM KOH; pH 7.2 External solutions contained K_2SO_4 or a combination of K_2SO_4 and Na_2SO_4 totalling 63 mM; 8 mM $CaSO_4$; 5 mM $MgSO_4$; 10 mM HEPES; 3 mM KOH; 70 mM sucrose; 30 μM strophanthidin; pH 7.2. Cs_2SO_4, in the range 0.125 mM - 0.5 mM, was added to external solutions. The ratios between inward currents through the K^+ inward rectifier in the presence and in the absence of Cs (R=I with Cs/I without Cs) were plotted against membrane potential. A four-fold decrease in external K^+ concentration shifted these curves about 20 mV to the left along the V_m axis, such that at a given V_m the fraction of current not blocked by Cs^+ was always greater in the lower external K^+ concentration. At each external K^+ concentration, K_m, obtained from the equation $R=(1+[Cs^+]_o/K_m)^{-1}$, is membrane potential dependent; in 129 mM $[K^+]_o$, K_m was 10.2 mM at -60 mV and 1.2 mM at -109 mV. The slope of the plot of log K_m against membrane potential indicates that K_m changes 10-fold for a change of about 52 mV in V_m.

T-AM-C9 EFFECTS OF TRH ON MEMBRANE POTASSIUM CURRENTS IN CLONAL PITUITARY TUMOR CELLS. J.M. Dubinsky* and G.S. Oxford. (Intr. by M.M. Goldner). The Neurobiology Program, University of North Carolina, Chapel Hill, NC

The pituitary tumor cell lines, GH3 and GH4/C1 both possess two types of outward potassium current. $I_K(V)$ which activates rapidly and then inactivates, and $I_K(Ca)$ which activates slowly and is sensitive to Ca^{++}. Thyrotropin releasing hormone (TRH), which stimulates prolactin release in these cells, produces distinct changes in each of these K currents. Both membrane potential and ionic currents were monitored in both of these cell lines using the patch clamp technique in the whole cell configuration. In current clamp, pressure ejection application of 1uM TRH produces a 10-30 sec transient hyperpolarization followed by a 1-4 min. period of increased action potential frequency. In voltage clamp, TRH produces a transient increase in $I_K(Ca)$ which recovers its normal amplitude within the same 30 sec period as the hyperpolarizing response. Preliminary experiments on isolated outside-out membrane patches reveal no changes in the single channel conductance or in the probability of opening of single Ca-activated K channels after TRH application. No changes were detected in inward Ca or Ba currents in response to TRH. This suggests that the increase in $I_K(Ca)$ produced by TRH may be secondary to a rise in cytosolic Ca released from intracellular stores as measured by others (Gershengorn and Thaw, Endocrinology, 1983). TRH also produces a longer lasting decrease in $I_K(V)$ amplitude and slows its activation. This response persists for 1-4 min before returning to its original amplitude, paralleling the time course of increased action potential activity. This effect of TRH may represent a direct modulation of voltage-activated potassium channels. (Supported by NIH grant NS18788 to G.S.O.).

T-AM-C10 HALOGENATED FLUORESCEINS: A NEW AND POTENT CLASS OF K CHANNEL BLOCKERS.
Richard J. Bookman, Dept. of Physiology/G4, University of Pennsylvania, Phila, PA., 19104.

The action of fluorescein derivatives on the internally perfused, voltage clamped squid giant axon has been studied. In the dark, internal fluoresceins have a specific interaction with the voltage dependent K channel. The most potent dyes are those which are heavily halogenated, e.g.tetra-iodo, tetra-chloro fluorescein (Rose Bengal - RB). 1.0 μM RB modifies about 75% of the channels; this reaction proceeds slowly and is only partially reversible. The ON kinetics of the K^+ currents, as indicated by the approach to steady-state, are slowed by an order of magnitude. This is not true for the OFF kinetics which are approximately normal. After very brief repolarizations (100us - 1ms), they re-open with more nearly normal ON kinetics. After longer closing intervals the slow ON kinetics are re-established. These slow transitions lead to a pulse frequency dependent increase in current amplitude and speeding of ON kinetics. Illumination of a stained axon has two effects. With a halogenated dye present in micromolar amounts (either inside or outside), light makes the membrane leaky. However, if internal dye is washed out after the K^+ currents have been modified, light specifically destroys K channels as evidenced by the fact that the K^+ conductance is reduced, the kinetics of the remaining conductance appear normal, and there is no increase in the leak conductance. This channel demolition proceeds exponentially and requires the halogenated derivatives. An unhalogenated derivative, like 6-carboxy fluorescein, has a dark effect similar to RB (although much less potent) but there is no apparent light effect. This dye also has an interesting action on the Na channel: millimolar concentrations inside the axon reversibly block both ionic and gating current. Supported in part by a Grass Foundation Fellowship.

T-AM-C11 K CHANNELS IN HUMAN T LYMPHOCYTES. M.D. Cahalan*, T.E. DeCoursey*, K.G. Chandy & S. Gupta, Depts. of Physiology & Biophysics* and Medicine, Univ. of Calif., Irvine CA, 92717. Human T lymphocytes were studied using the gigaohm seal technique. The predominant ion channel was a K-selective channel closely resembling delayed rectifier channels of muscle and nerve. K currents recorded under whole-cell voltage clamp turn on upon depolarization with a sigmoid time course. In mammalian Ringer solution the K conductance is half maximal at about -30mV and the maximum conductance is typically 4nS, representing 250 conducting channels. The time to 1/2 peak current decreases monotonically between -30mV and +80mV from about 30msec to 2msec. Under maintained depolarization the K current inactivates exponentially with a time constant that is only slightly voltage-dependent, of about 200msec at V>0mV, increasing at more negative potentials. Steady-state inactivation measured by changing the holding potential is describable by a Boltzmann distribution with a midpoint around -60mV and a slope of about 10mV. The selectivity of the K channel is similar to that of delayed rectifier channels of muscle and nerve. Relative permeabilities estimated from the change in reversal potential upon equimolar replacement of 160mM K^+ Ringer are: K^+ 1.0, Rb^+ 0.78, NH_4^+ 0.10, Cs^+ 0.03 and Na^+ 0.01. Upon changing from normal 4.5 K^+ to 160 K^+ Ringer, the maximum conductance approximately doubles, reflecting the behavior of single K channels. The unitary conductance at 0mV was about 16pS in 4.5 K^+ and 25pS in 160 K^+ Ringer. Single channel events recorded in outside-out patches or in whole cell conformation reveal complex gating kinetics. Unitary currents are frequently interrupted by rapid flickery closures. Changing the internal free calcium concentration from $2X10^{-9}$ M, the value in our standard KF pipette solution, to 10^{-8} M or 10^{-7} M by Ca-EGTA buffering of K aspartate solutions had no discernible effect on the voltage dependence of the K channel. When all internal K^+ was replaced by Cs^+ (aspartate) no macroscopic currents were observed in 3 lymphocytes. Supported by NIH grant # NS14609.

T-AM-C12 PHARMACOLOGY OF HUMAN T LYMPHOCYTE K CHANNELS. T.E. DeCoursey*, K.G. Chandy, S. Gupta & M.D. Cahalan*. Depts. of Physiology & Biophysics* and Medicine, Univ. of Calif., Irvine, CA 92717.

The voltage-gated K channel in human T lymphocytes displays pharmacological sensitivity to delayed rectifier K channel blockers, but the K current is also reduced by agents that block calcium channels and calcium-activated K channels. T lymphocytes in mammalian Ringer solution were voltage clamped using gigaohm seal technique in the whole cell configuration. The cells were held at -80mV and pulsed briefly to +20mV each 30 sec. The current remaining in the presence of the K channel blockers could be described by a one-to-one blocker-channel interaction. Half inhibition, K_i, occurred with 8mM tetraethylammonium (TEA) and 0.19mM 4-aminopyridine (4AP). Quinine, which has been used to block calcium-activated K channels, is also a potent inhibitor of T lymphocyte K channels with K_i=14 μM. Calcium channel antagonists inhibit K current in T lymphocytes. Verapamil, nifedipine and diltiazem all produce use-dependent block of K currents. Verapamil is the most potent, with K_i about 5μM for steady-state block, studied as described above. K channel block was relieved by witholding test pulses or by holding the cell at a more negative potential. This latter phenomenon is only partially due to relief of steady-state inactivation, since fewer than 20% of the channels are inactivated at -80mV. Polyvalent cations reduced peak K currents by several mechanisms: the voltage dependence of channel activation is shifted to more positive potentials, the maximum conductance is decreased, and in some cases inactivation occurs more rapidly. The concentrations required for these effects varied widely. The potency sequence for reducing the maximum K current is $La^{+++} > Zn^{++}, Co^{++}, Cd^{++} > Ba^{++} > Mn^{++} > Ca^{++} > Sr^{++} > Mg^{++}$. TEA, 4AP, quinine, diltiazem and verapamil inhibit phytohemagglutinin-induced mitogenesis in T lymphocytes in a sequence parallel to that for K channel block. Supported by NIH grant # NS14609 and a fellowship to KGC fron the American Diabetes Assoc., So. Cal. Affiliate.

T-AM-D1 ANESTHETIC-MEMBRANE INTERACTION AS VISUALIZED BY DEUTERIUM AND PHOSPHORUS NMR. Ian C.P. Smith, Eric C. Kelusky, and Michael A. Pass, Division of Biological Sciences, National Research Council, Ottawa, Canada K1A 0R6.

Since the turn of the century, anesthetic potency has been correlated with the solubility of the compounds in oil. However, the molecular mechanism of anesthesia has evaded clarification up to the present. Deuterium NMR of specifically-labelled anesthetics and lipids has yielded detailed information about the influence of anesthetics on lipids, the location of membrane-bound anesthetics, and the dependence of lipid-anesthetic interaction on the nature and charged state of the anesthetic. Data will be reported for the local anesthetics tetracaine and procaine interacting with model membranes of phosphatidylcholine and phosphatidylethanolamine, as well as with bovine spinal cord.

T-AM-D2 THREE-DIMENSIONAL STRUCTURE OF THE Ca^{2+} ATPase FROM SARCOPLASMIC RETICULUM. Kenneth Taylor[1], Laszlo Dux[2] and Anthony Martonosi[3]. [1]Dept. Anat., Duke Univ. Med. Ctr., Durham, N.C., 27710. [2]Inst. Biochem. School of Medicine, Univ. of Szeged, Hungary, [3]Dept. Biochem., SUNY Upstate Medical Center, Syracuse, N.Y., 13210.

The structure of the Ca^{2+} transport ATPase from skeletal muscle sarcoplasmic reticulum has been determined from crystalline tubules formed from native membranes using sodium vanadate. Analysis of the in-plane projection of crystalline tubules flattened onto carbon support film shows that the structure consist of ribbons of Ca^{2+} ATPase dimers that form right-handed helical tracks around the surface of the cylinder. The projection symmetry is P2, establishing that the crystals are made up of dimers of the enzyme.

We have recently extended the projected structure to a preliminary 3-dimensional density map that shows primarily the cytoplasmic part of the molecule. This portion of the molecule is roughly pear-shaped with a volume of about 85000Å^3. No density was observed protruding into the luminal space of the cylinders despite the accessibility of this region to negative stain. Some evidence of stain penetration within the bilayer was observed. The bonding of Ca^{2+} ATPase molecules to form the dimer creates a bridge over one side of the membrane. The bonding of dimers to form a chain is carried out through a lobe extending along the "a" axis of the crystal. This connection, however, is located near the surface of the bilayer. This research was supported by NIH grants GM/AM 28224, GM 30598, AM 26545 and grants from the Muscular Dystrophy Association.

T-AM-D3 INTERACTIONS BETWEEN PHOSPHOLIPID AND THE CA-ATPASE OF THE SARCOPLASMIC RETICULUM IN NATIVE AND RECOMBINED MEMBRANES. Barry S. Selinsky and Philip L. Yeagle. Department of Biochemistry, SUNY/Buffalo, School of Medicine, Buffalo, NY 14214.

Phosphorus nuclear magnetic resonance (NMR) spectra of sarcoplasmic reticulum membranes from rabbit muscle and of recombined membranes containing the Ca-ATPase of sarcoplasmic reticulum reveal two distinguishable, overlapping resonances. One resonance resembles a normal phospholipid bilayer resonance, and the other is much broader. The broader component is not seen in protein-free phospholipid vesicles. In recombined membranes of the Ca-ATPase, the intensity found in the broad component was proportional to the concentration of protein in the vesicles. The two component spectra are interpreted to arise from at least two different domains of phospholipids, one of which is motionally restricted by the Ca-ATPase. In light and heavy fractions of native sarcoplasmic reticulum, the number of phospholipids motionally restricted by the Ca-ATPase is modulated differently by potassium ions. The NMR results correlate with changes in the calcium transported/ATP hydrolyzed coupling ratio. In light sarcoplasmic reticulum, the coupling ratio increases with increasing potassium ion concentration, while in the heavy fraction the coupling ratio decreases with increasing potassium ion concentration. These results indicate that membrane phospholipid headgroups interact with the Ca-ATPase in sarcoplasmic reticulum membranes.

T-AM-D4 MORPHOLOGY OF PROTEOLIPOSOMES RECONSTITUTED WITH PURIFIED LAC CARRIER PROTEIN FROM E. COLI. M.J. Costello, D.L. Foster, P. Viitanen, N. Carrasco and H.R. Kaback, Dept. Anatomy, Duke Univ. Med. Cent., Durham, N.C. 27710 and Roche Inst. Mol. Biol., Nutley, N.J. 07110.

The lactose transport protein, lac carrier, purified from E. coli plasma membranes has been previously incorporated into E. coli lipid extracts using octylglucoside solubilization followed by freeze-thaw/sonication (Newman et al., 1981, J. Biol. Chem. 256: 11804). Freeze-fracture-etch electron microscopy was used here to characterize suspensions of proteoliposomes which were ultra-rapidly frozen in the absence of cryoprotectants (Costello, 1980, SEM 2: 261). Nearly all vesicles are unilamellar and the majority fall within the range of 300-1500 Å diameter. Pure lipid vesicles produce only smooth fracture faces, while proteoliposomes reconstituted with lac carrier produce 80-90 Å globular particles uniformly distributed on both convex and concave fracture surfaces. Reducing the protein-to-lipid ratio proportionately reduces the number of particles per unit area of lipid bilayer fractured. Rotary shadowing does not reveal a characteristic substructure within the particles, but their size suggests that each particle, correcting for the thickness of deposited metal, is probably composed of either one or two 46K dalton monomers. Etched surfaces of the vesicles are smooth, indicating that major portions of the transmembrane protein do not extend far from the bilayer surfaces, as predicted by a recent model of the secondary structure (Foster et al., 1983, J. Biol. Chem. 258: 31). Bivalent monoclonal antibody labeling of protein on the outside of the vesicles does not alter the size and shape of particles on concave fracture faces. These proteoliposomes are ideal for relating morphology to transport functions. Supported in part by NIH grant GM 27914 (to MJC).

T-AM-D5 NANOSECOND EMISSION ANISOTROPY MEASUREMENTS OF THE EFFECT OF BEE VENOM MELITTIN ON THE ORGANIZATION AND DYNAMICS OF DIMYRISTOYLPHOSPHATIDYLCHOLINE BILAYER LIPOSOMES. S. Georghiou and T. Bradrick, Biophysics and Chemical Physics Lab., Department of Physics, University of Tennessee, Knoxville, TN 37996-1200

The interaction of melittin, the major protein component of bee venom, with dimyristoylphosphatidylcholine bilayer liposomes has been investigated by employing the technique of nanosecond emission anisotropy with 1,6-diphenyl-1,3,5-hexatriene (DPH) as the fluorescent probe. DPH, a rod-like molecule, has its absorption and emission dipole moments along its long axis and reports on the conformation and motions of the acyl chains of phospholipids. The technique has high information content yielding separately the order parameter, S, and the rotational correlation time, ϕ. This is contrasted with steady-state fluorescence polarization measurements that are usually interpreted in terms of "fluidity", an ill-defined term. We find that the major effect of melittin is exerted in the liquid-crystalline phase of the bilayer where it increases S by a factor of about 1.8 and decreases ϕ by a factor of about 3.5. Thus, the protein decreases the amplitude and increases the rate of motion of the acyl chains. Using the wobbling-in-a cone model, we find that the average direction of the emission transition dipole moment of DPH makes an angle of 27° with the normal to the bilayer surface in the presence of 1/45 melittin-to-lipid molar ratio and 40° in the absence of melittin. These findings imply that melittin exerts pronounced effects on the organization and dynamics of the phospholipid whose functional implications will be discussed. (Supported in part by grant RR-07088 of the Biomedical Program of NIH).

T-AM-D6 PROTEIN ROTATIONAL MOTION IN SOLUTION AND SINGLE CELLS MEASURED BY POLARIZED FLUORESCENCE DEPLETION. T.M. Yoshida and B.G. Barisas, Dept. of Chem., Colorado State Univ. Ft. Collins, CO 80523

A new microscope-based system directly measures protein rotational motions in viscous environments like cell membranes by polarized fluorescence depletion (PFD). The method is very similar to a technique introduced by Garland. Proteins labeled with fluorophores such as eosin (EITC) having high quantum yields for triplet formation are examined anaerobically in a fluorescence microscope. An acoustooptic modulator generates ~ 10 μsec x 20 mW pulses of linearly polarized 514 nm light which produce an orientationally-asymmetric depletion of ground state fluorophores in the sample. When the sample is probed with 0.1 mW light polarized $\parallel$ to the exciting pulse, fluorescence recovers over 0-1000 μsec as the sum of two exponentials. One corresponds to the triplet liftime τ_L and the other to the rotational relaxation time τ_R of fluorophores into the depleted orientation. In alternating cycles an exciting pulse $\perp$ to the probe beam is used. Fluorescence recovery is then the difference of the exponentials. Data are collected with a Nicolet 12/70 signal averager and analyzed on-line according to one of three models: 1) isotropic 3-D rotation 2) 2-D rotation normal to optical axis 3) 2-D rotation of objects located around the surface of a sphere. τ_R down to 10 μsec are measured and 200,000 EITC molecules yield an excellent signal. A sliding optical table permits photobleaching recovery measurements of lateral diffusion coefficients D_T in the same microscope. EITC-BSA in 99% glycerol at 9° has τ_R = 130.3 μsec while theory predicts 125 μsec. Plotting $1/D_T$ vs τ_R for the sample at various temperatures T yields a straight line of unit slope. This plot cancels uncertainties in T and in solvent viscosity η and demonstrates that τ_R is indeed proportional to η. Thy 1.2 antigen rotation on groups of 10-20 murine T cells has been measured. Single cells and other membrane proteins are under study. Supported by grants NSF PCM 81-11385 and NIH AI 00506.

T-AM-D7 DISTANCE ESTIMATE OF THE ACTIVE SITE OF D-β-HYDROXYBUTYRATE DEHYDROGENASE [BDH] WITH RESPECT TO THE MEMBRANE SURFACE. Lauraine Dalton, J. Oliver McIntyre and Sidney Fleischer. Department of Molecular Biology, Vanderbilt University, Nashville TN 37235.

BDH is a lipid-requiring enzyme which has been purified to homogeneity. The enzyme devoid of lipid is inactive but can be reactivated by insertion into phospholipid vesicles containing lecithin. BDH inserted into mitochodrial phospholipid vesicles (BDH-MPL) is indistinguishable from the membrane-bound enzyme in submitochondrial vesicles. BDH-MPL was selectively derivatized with spin label (SL) [4-maleimido-2,2,6,6-tetramethylpiperidinooxyl] so as to obtain unique site labeling of the essential sulfhydryl. SL-BDH-MPL was titrated with paramagnetic transition ions, e.g., Mn^{2+}, Co^{2+}, Cu^{2+}, Cu-EDTA^{2-} or Gd^{3+} until a limiting reduction in EPR signal amplitude was obtained. The limiting reduction of amplitude afforded by each ion was calibrated by titrating MPL liposomes containing spin-labeled lecithin with the nitroxide moiety at the 5-, 12-, and 16-carbons of the sn-2 fatty acyl chain. From the relative amplitude in the presence vs absence of transition ions, the radial distance, r, between the nitroxide group of the SL and the transition ions in aqueous media was calculated according to the formalism of Leigh [Leigh, J.S., (1970), J. Chem. Phys. 52, 2608], i.e., the limiting reduced amplitude affords a measure of the dipolar interaction coefficient, which is proportional to $1/r^6$. The direct calculations using different transition ions and the empirical calibration methods both give similar values. For BDH in the membrane, we find that the SL on the essential sulfhydryl in the vicinity of the active site is located 8-10 Å from the aqueous domain. [Supported by NIH AM 21987]

T-AM-D8 EVIDENCE FOR DIRECT INSERTION OF FRAGMENTS A AND B OF DIPHTHERIA TOXIN INTO MODEL MEMBRANES. Valerie W. Hu and Randall K. Holmes, Departments of Biochemistry and Microbiology, Uniformed Services University, 4301 Jones Bridge Road, Bethesda, Maryland USA 20814

The receptor-independent entry of diphtheria toxin into model membranes was studied using a membrane-restricted photoprobe to monitor insertion. With negatively-charged liposomes, optimal binding was achieved at pH 3.6 and at room temperature. Under these conditions, the A and B domains of nicked as well as unnicked toxin were inserted. At 0 °C, optimal binding of toxin and insertion of fragment B occurred, but fragment A remained exposed at the surface of the liposomes. At neutral pH, there was very little binding of toxin and fragment B was preferentially inserted. This pH-dependent difference in binding and insertion did not result from a requirement for a pH gradient across the membrane. Brief exposure of the toxin to pH 3.6 followed by a return to pH 7 and subsequent incubation with vesicles at neutral pH greatly facilitated binding and resulted in insertion of both fragments. We interpret this pH effect primarily as an indication of a pH-induced conformational change in the toxin which exposed hydrophobic residues and resulted in increased membrane interaction. There was little binding of toxin with neutral vesicles at pH 3.6 suggesting a role for membrane surface charge in toxin binding. These results indicate that insertion of diphtheria toxin into membrane vesicles may involve two sequential conformational changes, a pH-induced change that facilitates insertion of the B domain into negatively-charged membranes and a subsequent temperature-dependent change leading to direct insertion of fragment A into the lipid milieu.

T-AM-D9 FORCES BETWEEN INTRINSIC MEMBRANE PROTEINS BY THE ANALYSIS OF FREEZE-FRACTURE ELECTRON MICROGRAPHS: GAP JUNCTIONS, Jochen Braun, James R. Abney, and John C. Owicki, Dept. of Biophysics and Medical Physics, University of California, Berkeley, CA 94720.

The lateral distribution of membrane proteins is a functionally significant aspect of membrane structure. We have studied gap junctions with the aim of understanding how the lateral distribution of the connexons arises. Assuming that pair forces between connexons govern their lateral distribution, we have devised a computer-based method of analyzing electron micrographs to obtain the magnitude and functional form of such forces. Our method employs the Born-Green-Yvon (BGY) hierarchy, an integral equation from the statistical-mechanical theory of liquids that relates correlation functions for n and n+1 particles to the distance-dependent forces between particles (T.L. Hill, Statistical Mechanics (1956) McGraw-Hill, N.Y., Chapt. 6). Pair and triplet correlation functions can be computed from freeze-fracture electron micrographs of rapidly frozen membranes; such micrographs approximate the instantaneous positions of proteins in the native membrane. Rotationally averaged forces can then be obtained via the BGY integral equation. Integration of the forces yields the effective pair potential-energy function. This includes both direct and indirect (e.g., lipid-mediated) interactions. For gap junctions from mouse liver in the conducting conformation (micrographs a generous gift of E. Raviola; E. Raviola et al. (1980) J. Cell Sci. 87:273), we find effective forces of a range of about 12nm that are purely repulsive. The observed pair forces thus cannot account for the cohesion of connexons in gap junctions; any forces responsible for this aspect of the lateral distribution must be analogous to a lateral pressure. An effective pressure could arise, e.g., from non-pairwise-additive lipid-mediated interactions between the proteins, or from the minimization of repulsions between the closely apposed cell membranes. Supported by NIH BRSG #2-S07-RR07006 and ACS/PRF #12378-G6 grants.

T-AM-D10 MONOGALACTOSYLDIACYLGLYCEROL AT AIR-WATER INTERFACE. Rami Almog and Donald S. Berns, Center for Laboratories and Research, New York State Department of Health, Albany, New York 12201

The association of phycocyanin (an algal membrane-protein) with dipalmitoyl phosphatidylcholine (DPPC) and monogalactosyldiacylglycerol (MGDG) was investigated. A stronger interaction with MGDG was indicated. However, at air-water interface, MGDG monolayer underwent a rapid oxidation leading to aqueous soluble degradation products and elimination of the monolayer from the interface. The presence of phycocyanin or DPPC at the air-water interface did not affect the oxidation process. MGDG was reported to stabilize photosynthetic Black Lipid Membranes. Other components, such as chlorophyll, must therefore inhibit the oxidation of MGDG in these membranes.

T-AM-E1 THE SPECIFIC ATPASE ACTIVITY OF V_1 MYOSIN CHANGES IN THE MATURING RAT HEART. R. Horowits and S. Winegrad, Dept. of Physiology, University of Pennsylvania, School of Medicine, Phila., PA

An immunohistochemical technique was developed for quantitating cellular myosin isozyme composition in sections of rapidly frozen rat ventricles. 6 μ thick sections of ventricles from neonatal to 12 month old rats were stained with affinity purified anti-V_1 antibody by a modification of Sternberger's unlabeled antibody peroxidase-antiperoxidase technique (L.A. Sternberger, Immunocytochemistry, 2nd edition (John Wiley and Sons, N.Y., 1979), pp. 104-169). In each section the absorbance of a 3.17 μ spot in each of 30 cells was determined, and the results were averaged to give a mean value for the absorbance of that section. The amount of V_1 heavy chain in an unsectioned portion of each ventricle was determined by native gel electrophoresis, and was linearly related to the intensity of antibody staining ($r = 0.86$). The variability of V_1 concentrations measured in individual sections is relatively small and gives no indication of more than one population of cells. The relative specific activity of V_1 ATPase was calculated from measurements in serial sections of V_1 heavy chain concentration and V_1 myosin ATPase activity. The specific activity of V_1 in tissue sections remains relatively constant for the first month of life, but increases by approximately 50% from 1 to 4 months; the average specific activity of V_1 remains at this increased level until over 1 year of age. These observations are consistent with the early appearance in the heart of a system for directly regulating the activity of V_1 myosin. (Supported by grant NHLBI 15835)

T-AM-E2 CYCLIC AMP REGULATION OF CARDIAC MYOSIN ATPASE. S. Winegrad and A. Weisberg, Dept. of Physiology, University of Pennsylvania, School of Medicine, Phila., PA

The enzymatic activity of cardiac myosin has been studied in cryostatic sections of quickly frozen rat hearts in order to minimize post mortem changes in the cells. Ca and actin-activated ATPase has been measured histochemically (Weisberg et al., Circul. Res. 51, 802, 1982). The specificity of the technique for measuring myosin ATPase was shown by: 1)the localization of reaction product in the A bands; 2)the constancy of Ca-activated ATPase with changes in sarcomere length between 2.0 and 3.0 μ; and 3)the gradual decrease in concentration of reaction product of actin-activated ATPase with increasing sarcomere length. The ability of the technique to make quantitative measurements was supported by: 1)linearity of phosphate production with time; 2)approximate linearity with section thickness; and 3)saturation with increasing concentration of ATP and a Km similar to values in the literature. Addition of cAMP and theophylline increased both Ca and actin-activated myosin ATPase in 16 hearts from young, euthyroid rats with predominately V_1 isozyme of myosin by 52 ± 6%. Myosin ATPase activity of hearts from hypothyroid rats, in which myosin is entirely V_3 isozyme, was approximately 60% of the value in euthyroid hearts, and cAMP and theophylline reduced myosin ATPase by 42 ± 4%. Myosin ATPase activity was increased in a dose-related manner in isolated perfused hearts from young, euthyroid hearts by the addition of isoproterenol to the perfusion medium. These results show that myosin regulation by a cAMP-sensitive mechanism can be demonstrated in cardiac tissue that has been quickly frozen to preserve normal structure. (Supported by grant NHLBI 15835)

T-AM-E3 COMPARISON OF VENTRICULAR MYOSIN SUBFRAGMENT I ISOENZYMES PREPARED FROM ADULT AND FETAL HUMAN HEARTS. L.S. Tobacman and R.S. Adelstein, Laboratory of Molecular Cardiology, National Heart, Lung, and Blood Institute, NIH, Bethesda, MD 20205.

Human adult and fetal cardiac myosin are known to differ in light chain (LC) composition. At 14-17 weeks gestational age 40% of the fetal cardiac myosin alkali light chains migrate on SDS PAGE at 28,000-dalton M_r (LC_{1f}). The remainder of the fetal alkali LC and all of the adult alkali LC migrate at 27,000-dalton M_r (LC_{1a}). In contrast to cardiac myosin from many mammalian species, human cardiac myosin heavy chains from adult and fetal ventricles are indistinguishable and possibly identical. In order to compare the function of fetal and adult myosin, we prepared chymotryptic subfragment 1 (S_1) from fetal and adult hearts. The fetal S_1 was separated by DEAE cellulose chromatography into two isoenzymes, containing either LC_{1f} or LC_{1a}. At 25°C, 15mM MOPS, 2mM $MgCl_2$, 1mM ATP, 0.1mM EGTA, 0.1mM DTT, pH 7.0, the actin-activated Mg^{2+}ATPase rates of the S_1 preparations were compared. Fetal S_1 containing LC_{1f} had a Km of 11uM actin and a Vmax of $4.3s^{-1}$, while fetal S_1 containing LC_{1a} had a Km of 11uM and a Vmax of $4.0s^{-1}$. The Km and Vmax of S_1 from the adult heart were 14uM actin and $5.7s^{-1}$. These data indicate that the fetal cardiac LC_1 does not alter the ATPase rate of myosin heads and presents the first direct comparison of myosin isoenzymes derived from human hearts.

T-AM-E4 STRUCTURAL CHANGES IN SCALLOP MYOSIN FILAMENTS ON CALCIUM ACTIVATION
Roger Craig[+] and Peter Vibert[*]. [+]Department of Anatomy, University of Massachusetts Medical School, Worcester, MA 01605 and [*]Rosenstiel Center, Brandeis University, Waltham, MA 02254.

Scallop striated muscle is activated by binding of Ca^{2+} to the myosin crossbridges, but little is known of the structural events occurring upon activation. Thick filaments isolated in relaxing solutions invariably retain an ordered helical surface array of crossbridges when negatively stained (Vibert & Craig, J. Mol. Biol. 165, 303-320 (1983)). When the filaments are treated briefly with Ca^{2+}-containing activating solutions before staining, the appearance of the surface array is altered. The oblique striping characteristic of alignment of crossbridges along helical tracks is weakened, although the strong 145 Å axial periodicity is retained. Longer treatments produce disorder; the bridges are apparently clumped together on the filament surface, but 145 Å periods are still visible in some cases. Occasionally, thin filaments lie alongside the thick filaments, an appearance not seen in relaxed samples. Attempts to reverse these structural changes by a further treatment with relaxing solution before staining have been partially successful. Some filaments regain a more ordered helical appearance while others remain disordered. These initial results suggest a specific structural change in the thick filaments in response to the binding of Ca^{2+} ions by the myosin crossbridges, although we have not ruled out the possibility of non-specific effects during longer activations.
Supported by grants from NSF, NIH and MDA.

T-AM-E5 SKELETAL MYOSIN FILAMENT FORMATION *IN VITRO*: LENGTH DETERMINATION.
F.A. Pepe, B. Drucker and P. Chowrashi, Dept. of Anatomy, Univ. of Pennsylvania, Philadelphia, Pa 19104

The formation of myosin filaments from myosin solutions by reducing the ionic strength of the solution gives filaments structurally similar to native filaments but with a wide distribution of lengths (Huxley, J.M.B. 7:281-308, 1963). Native filaments separated from skeletal muscle have a precisely determined length of about 1.5μm (Morimoto & Harrington, J.M.B. 77:165-175, 1973). We have identified some of the conditions required to produce synthetic filaments with lengths of about 1.5μm which approach the precision of length determination found in native filaments. We have found that certain portions of the myosin eluted from DEAE Sephadex A-50 produce filaments with the sharpest length determination at 1.5μm. Using this myosin we studied the effect of a) protein concentration; b) pH; c) KCl conc.; and d) rate of change of KCl conc. on filament length distribution. It was found that the rate of change of KCl conc. was the most critical parameter for length determination and that the rate required from 0.6 to 0.3M KCl was different than the rate required from 0.3 to 0.15M KCl. In the range from 0.3 to 0.15M, the critical region was found to be from 0.3 to 0.28M. On reaching 0.28M KCl, changing the rate of change of KCl conc. did not affect the length distribution obtained at 0.15M KCl. The effect of PH and protein concentration on filament lengths was similar to that described previously by Katsura and Noda (Adv. Biophys. 5:177-202, 1973) in that the filaments decreased in length on either side of pH7. The length of the filaments as a function of KCl conc. was similar to that described for native filaments (Trinick & Cooper, J.M.B. 141: 315-321, 1980) in that from 1.6μm to 1.4μm there was a small change in length with change in KCl conc., and then a steeper change from 1.4μm to 0.4μm (at 0.3M KCl). This suggests that the synthetic filaments are structurally similar to native filaments.

T-AM-E6 SMOOTH MUSCLE MYOSIN MINIFILAMENTS.
Kathleen M. Trybus and Susan Lowey. Rosenstiel Center, Brandeis University, Waltham, MA 02254.

Dephosphorylated smooth muscle myosin filaments (pH 7.5/0.15 M KCl) are depolymerized by stoichiometric amounts of MgATP to a far greater extent than filaments in which the 20,000 dalton light chain is phosphorylated. To determine if the difference in filament stability is due to a difference in myosin packing, the conformation of "minifilaments" prepared from dephosphorylated and thiophosphorylated myosin was examined by sedimentation velocity and electron microscopy. Unlike filaments formed in 0.15 M KCl, minifilaments are highly homogeneous aggregates of <20 molecules, similar to those described for skeletal muscle myosin. Different size minifilaments (15S-25S) can be obtained by varying either the pH of the solvent or the concentration of citrate/tris buffer. In the absence of MgATP, phosphorylated and dephosphorylated minifilaments (5 mM citric acid/22 mM tris) sedimented at the same rate (s^{o}_{20w}≈22S), indicating that the polymers are similar in size and shape. Consistent with this finding, the rod alone forms minifilaments, suggesting that the head does not play a major role in the assembly of these aggregates. Upon addition of 1 mM MgATP, however, the phosphorylated minifilaments remained polymerized, but the dephosphorylated minifilaments were dissociated to a 15S species. The broadness of the 15S boundary distinguished it from the hypersharp minifilament peak. A similar 15S species (0.05 M KCl) was shown by electron microscopy to be an antiparallel dimer of myosin in which each subunit is in the folded 10S conformation. These results suggest that differences in stability between phosphorylated and dephosphorylated filaments are largely due to conformational changes occurring in the head region of myosin as a result of phosphorylation and nucleotide binding.

T-AM-E7 C-PROTEIN AND MYOSIN FILAMENT ASSEMBLY

Julien S Davis, Department of Biochemistry, Witwatersrand University, Johannesburg, 2001, South Africa.

Myosin from skeletal muscle assembles by the addition of 44 nm dimer to filament at a rate independent of length. The dissociation rate constants on the other hand increase exponentially as the filament grows from the bare-zone out to its full-length. Growth ceases at the point of equilibrium between the 'on' and 'off' rates (Davis, J.S. (1981) Biochem. J. 197, 309-314). The structural role of copolymerizing proteins has been elucidated by observing their effect on this basic mechanism and some results with C-protein are presented here.

The addition of C-protein increased the length of the filaments and stabilized them against dissociation by pressure. Pressure-jump experiments revealed that the assembly reaction slowed to a minimum at a 1:1 ratio of the proteins. Similar results were obtained for the dissociation reaction when carried out a few seconds after the completion of assembly. These effects can be ascribed to the binding of C-protein in a potential 1:1 stocheiometry to the S-2 region of myosin in monomer, dimer and filament. This is essentially a passive role, having virtually no effect on filament length. The rate of dissociation however declined further in an exponential fashion as the time after assembly increased. An analysis of these data revealed that C-protein had little effect on the intrinsic cooperativity of myosin assembly but did slow down the overall rate of dissociation. These binding sites which are additional to the S2 sites are thus equivalent and independent of the underlying length-regulation mechanism, and their occupation results in an increase in filament length. The exponential form of the kinetics implies the existence of a rate-limiting isomerization in the reaction process.

T-AM-E8 MYOSIN HEAD TOPOGRAPHY BY IMMUNO-ELECTRON MICROSCOPY. Donald A. Winkelmann and Susan Lowey, Rosenstiel Research Center, Brandeis University, Waltham, MA 02254.

Monoclonal and polyclonal antibodies which react with defined regions of the heavy and light chains of chicken skeletal myosin have been used to provide a correlation between the primary sequence and the structure of the molecule. The monoclonal antibodies react with several epitopes in the 25kd and 50kd tryptic fragments of myosin S1, and the amino terminus of the LC2 light chain (Winkelmann, Lowey and Press (1983) Cell 34, 295-306); the polyclonal antibodies are specific for the amino terminal sequences of LC1 (anti-$\overline{\Delta 1}$) and LC3 (anti-$\Delta 2$) light chains (Silberstein and Lowey (1981) J. Mol. Biol. 148, 153-189). Each of these antibodies was found to bind to myosin, and the site of attachment was localized by electron microscopy of rotary shadowed complexes. All of the antibodies to the 25kd and 50kd head domains map to the thick portion of the myosin head at a distance greater than 140 Å from the head-rod junction. These antibodies bound to the heads in several orientations, suggesting that each of the heads is able to independently rotate 180° about the head-rod junction. Monovalent Fab fragments of the anti-25kd antibodies were also used to probe the accessibility of these epitopes on S1-decorated actin and demonstrate that these epitopes are not on the contact surface between S1 and actin. The antibodies specific for the amino termini of both classes of myosin light chains map to the neck region of the head within 90 Å of the head-rod junction. This location is similar to that found for the regulatory and essential light chains on scallop myosin by Flicker et al. (1983, J. Mol. Biol. 169, 723-741); our data extend these findings by localizing the amino termini of both classes of light chains. (Supported by grants from NIH, NSF, the Muscular Dystrophy Assoc., and The Medical Foundation, Inc.)

T-AM-E9 FAST SKELETAL MYOSIN DENUDED OF LC2 BY IMMUNOADSORPTION. S.C. Pastra-Landis and Susan Lowey. Rosenstiel Center, Brandeis University, Waltham, MA 02254.

The 20K dalton light chain (LC2) can be completely removed from chicken pectoralis myosin in 1mM EDTA and 5mM ATP by using immunoaffinity chromatography. The immunoadsorbent, prepared with antibody specific for LC2, was able to bind all the LC2 from a mixture of total light chains at 4°C. However, the light chain in intact myosin did not bind to this column at either 4°C or 25°C. Only at elevated temperatures (37° to 40°C) was the binding of the light chain to the myosin heads sufficiently weakened to permit its complete removal by the antibody. This has allowed the isolation of fast skeletal myosin denuded of all LC2, but otherwise native and not altered by chemical or protease treatment. The denuded myosin retained full enzymatic activity in K^+ and Ca^{++} ATPase media with velocities of 10.2 and 1.7 s^{-1} per head, respectively. Preliminary experiments with the actin-activated Mg^{++} ATPase did not show substantial differences in the kinetic parameters between native myosin and LC2 deficient myosin. Electron microscopy of rotary shadowed preparations of the LC2 denuded myosin showed it to have a marked tendency to aggregate at the head region into oligomers, in contrast to control myosin which appeared monomeric under identical conditions. An apparent "sticky" site is created on the head once the LC2 is removed, giving rise to a molecular distribution consisting of 50% dimers and trimers. This behavior is consistent with results from desensitized scallop myosin (Flicker et al., 1983) and from LC2 deficient myosin produced by controlled proteolysis (Margossian et al., 1983), which suggest that the LC2 is located in the neck region of the myosin head, adjacent to the S1/S2 junction.

T-AM-E10 EFFECT OF NUCLEOTIDES ON THE PROTEOLYSIS OF MYOSIN SUBFRAGMENT-1. D. Applegate and E. Reisler, Dept. of Chem. and Biochem. and the M.B.I., UCLA, L.A., CA 90024

Limited proteolytic digestions of myosin subfragment-1 with elastase, subtilisin, papain and thermolysin reveal that the two trypsin sensitive regions of S-1 possess broad protease susceptibility (in press). Cleavage by these enzymes produces peptide fragments which correspond within 1-2K daltons to the 25K, 50K, and 20K fragments produced by trypsin. While papain and thermolysin cut preferentially at the 26K/70K junctions, elastase and subtilisin cleave both the 26K/70K and the 75K/22K junctions in S-1. Using the above proteases as conformational probes we have previously demonstrated that the binding of actin is sensed at both the 26K/50K and the 50K/22K junctions. We report here that the binding of nucleotides at the active site is also sensed at both junctions. Both 2 mM MgADP and 5 mM MgATP slow the elastase and the subtilisin cleavage of the 95K heavy chain by a factor of 2. With elastase, the slowing is evidenced at both the 22K/50K and the 50K/26K junctions. The analysis of subtilisin digestions is complicated by Mg-nucleotide induced cleavage at a new site to produce 90K, 70K, 50K, and 22K fragments. Using MnsCl to fluorescently label the reactive lysine on the 26K peptide, we demonstrate that the additional cleavage site is approximately 5K daltons from the N-terminal of the 95K heavy chain. The binding of either 2 mM MgADP or 5 mM MgATP to S-1 caused a 2-fold increase in the rate of the thermolysin cleavage of S-1 at the 70K/26K junction but inhibited the cleavage at the same junction by papain. The above results demonstrate that the binding of MgADP and MgATP to S-1 is sensed at both the 26K/50K and the 22K/50K junctions of the 95K heavy chain. Supported by an AHA postdoctoral fellowship and grants from USPHS (22031) and MDA.

T-AM-E11 DIFFERENTIAL PROTEOLYSIS OF UNPHOSPHORYLATED RABBIT SKELETAL MYOSIN BY CA2+-ACTIVATED NEUTRAL PROTEASE. S.M. Pemrick and R.C. Grebenau. Dept. of Biochemistry, SUNY, Downstate Medical Center, Brooklyn, NY 11203.

Ca2+-activated neutral protease (CAF) was capable of degrading myosin over a wide range of protease concentrations (0.5 to 100 μg/ml at 5 mg/ml myosin). Time course experiments under conditions where native myosin and not partially degraded myosin was the substrate indicated that the reaction rate was limited by autodegradation of the 80K subunit of CAF. Multi-treatments with CAF spaced to account for CAF autodegradation gave no evidence for a low affinity of myosin for CAF. Although CAF selected for the heavy chain, high concentrations of CAF degraded L1 but not L2 nor L3. The following results demonstrated that CAF selected for the "head": 1) during the first hour, large fragments of identical Mr were produced from filamentous and from soluble myosin; 2) LMM was not a substrate; 3) actin, MgATP, and L2 had both a qualitative and quantitative effect on degradation; 4) myosin and HMM had similar cleavage sites although HMM was a poor substrate. The principal cleavage sites on native myosin were 20 (site 1), 35 (site 2), and 50 K (site 3) from the N-terminus to produce large fragments which retained normal intramolecular associations to comprise a "nicked" species of active myosin which may be of pathophysiological importance. Furthermore, differential degradation near site 3 indicated that L2 is near the ATP and the actin-binding domains. Supported by grants from NIH (HL22401) and MDAA.

T-AM-E12 OXYGEN EXCHANGE ACCOMPANIES ATP HYDROLYSIS CATALYZED BY ACTIVE AND RELAXED GLYCERINATED RABBIT PSOAS FIBERS. M.G.Hibberd*, M.R.Webb+, Y.E.Goldman* and D.R.Trentham+ Departments of Physiology* and of Biochemistry and Biophysics+ University of Pennsylvania, Philadelphia, PA 19104

With myosin and actomyosin, oxygen exchange can occur between phosphate and water during ATP hydrolysis. Oxygen exchange indicates that the ATP cleavage step is readily reversible and that the rate of ATP re-formation is rapid compared to the rate of P_i release. We have applied this technique to muscle fibers. Pairs of glycerinated rabbit psoas muscle fibers, mounted between a force transducer and a rigid support, were immersed in a 35 μl trough of relaxing solution including 15 mM ATP, $<10^{-8}$ M Ca^{2+}, 200 mM ionic strength, pH, 7.1 and 22°C. The solvent was 95% enriched with ^{18}O. Approximately 10% of the ATP was hydrolyzed after a 15 h incubation at which time the fibers were removed from the medium. Product P_i was isolated, converted to triethyl phosphate and analyzed for ^{18}O distribution by mass spectrometry. Most of the product P_i showed complete oxygen exchange. The distribution of ^{18}O atoms among the product P_i isotopes indicated more than one pathway for ATP hydrolysis as observed with soluble myosin. Thus the chemical pathway of the ATPase in relaxed fibers is similar to that of myosin in solution. The experiment was repeated with Ca^{2+} activated single fibers. In this case approximately 20% of the ATP was split in 2 h. Product P_i from active fibers showed much less oxygen exchange as might be expected since interaction with actin reduces the extent of oxygen exchange with soluble myosin. Although some contribution to the product P_i may have been due to non-actomyosin Ca-dependent ATPases in our experiments, the pattern of exchange for the majority of P_i molecules indicates quenching of oxygen exchange by cross-bridge attachment. Support: NIH grants HL15835, AM00745, AM23030 and MRC, U.K.